Supplementary

Effect of Microstructure on Coalescence-Induced Droplet Jumping Behavior of a Superhydrophobic Surface and Its Application for Marine Atmospheric Corrosion Protection

Zhengshen Chen [1,2,†], Xiaotong Chen [1,†], Yihan Sun [2,3], Guoqing Wang [1,*] and Peng Wang [2,3,*]

[1] State Key Laboratory of Marine Resource Utilization in South China Sea, School of Materials Science and Engineering, Hainan University, Haikou 570228, China; 21220856000009@hainanu.edu.cn (Z.C.); chenxiaotong161@163.com (X.C.)
[2] Key Laboratory of Marine Environmental Corrosion and Biofouling, Institute of Oceanology, Chinese Academy of Sciences, Qingdao 266071, China; sunyihan@qdio.ac.cn
[3] Center for Ocean Mega-Science, Chinese Academy of Sciences, Qingdao 266071, China
* Correspondence: wangguoqing@hainanu.edu.cn (G.W.); wangpeng@qdio.ac.cn (P.W.)
† These authors contributed equally to this work.

S1. The Mechanism of Microstructure Transformation

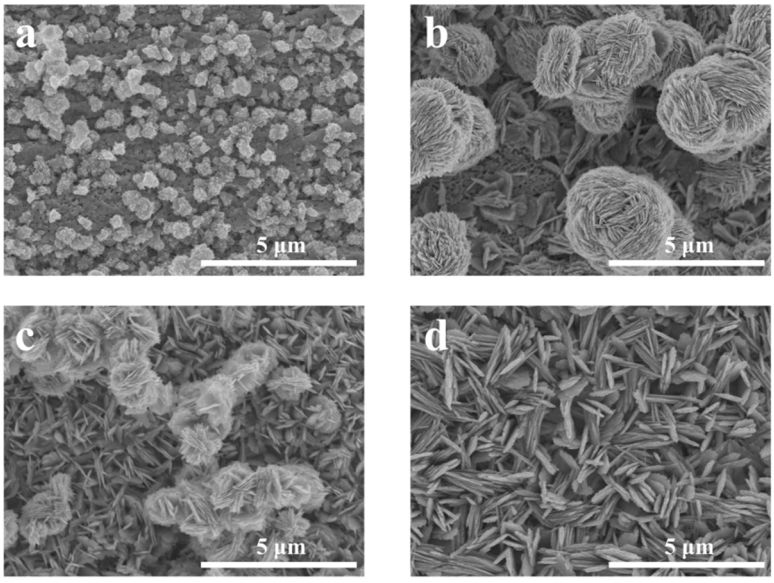

Figure S1. FE-SEM images of samples soaked in ammonia at 50 °C for (**a**) 24 h, (**b**) 48 h, (**c**) 60 h, and (**d**) 72 h.

According to SEM images of samples soaked at 50 °C for different times, as shown in Figure S1. We speculate that the copper oxide formed on the surface of the copper sheet will exist in the flower-like structure during the early stage of soaking in ammonia. As the reaction progresses, the oxygen and ammonia in the bottle are consumed, and the copper oxide

begins to form in a sheet structure. It can be seen that the sample after 48 h reaction is a micro-nano composite structure, the bottom layer is densely arranged with a diameter of about 60 ~ 100 nm nanosheets, and the top layer is a diameter of about 1 ~ 3.5 μm "flower" formed in the early reaction. After 60 h of reaction, it can be observed that the top "flower" begins to gradually fall off the nanometer. After 72 h of reaction, the bottom nanosheet grows to a diameter of about 90-150 nm, and the top "flower" completely falls off from the nanosheet, thus changing from a flower-like structure to a sheet structure.

S2. The Contact Angles (CAs) of the F-SS and S-SS after the Ammonia Immersion and Chemical Vapor Deposition.

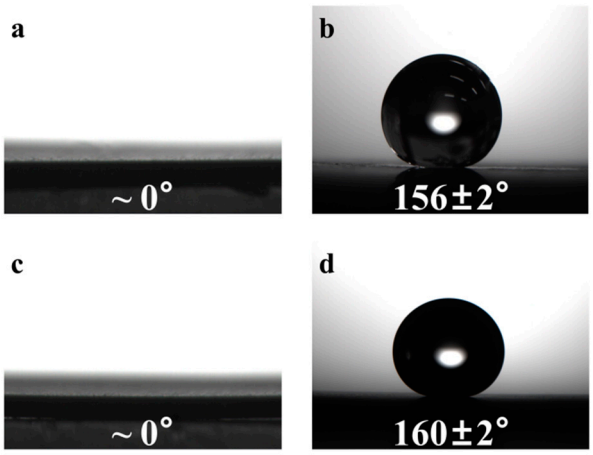

Figure S2. The CA of the (**a**-**b**) F-SS, and (**c**-**d**) S-SS after the ammonia immersion and chemical vapor deposition.

S3. FE-SEM Images of the Samples after the Simulated Condensation Experiments

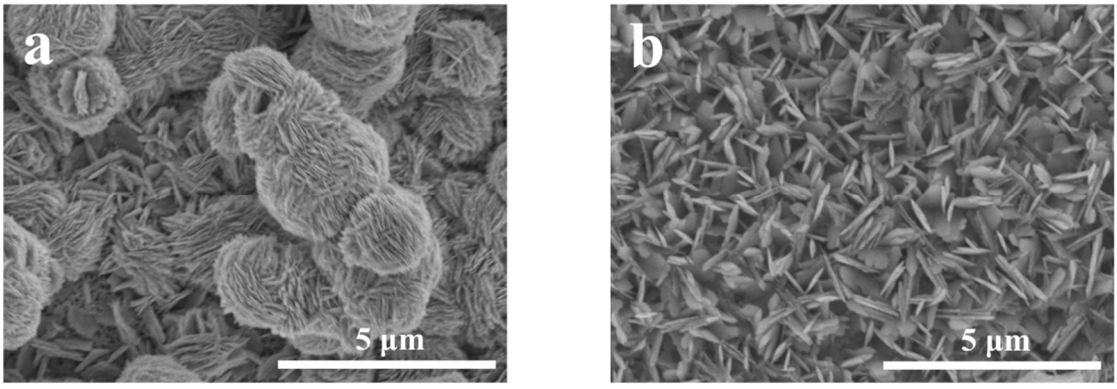

Figure S3. FE-SEM images of the (**a**) F-SS and (**b**) S-SS after the simulated condensation experiments.

We observed the surface morphology of the samples after the simulated condensation experiments, and the FE-SEM images were shown in **Figure S3**. Compared with FE-SEM images before condensation, no significant changes were found.

S4. Video of the Coalescence-induced Droplet Jumping behavior of the F-SS and the S-SS.

S5. Equivalent Circuits for the EIS Results

We used different equivalent circuit diagrams to fit the EIS results. In Bode-phase angle versus frequency plots, the high-frequency region and the low-frequency region correspond to the film layer and the corrosion interface layer, respectively [58]. Hence, a circuit (Figure S4a) is used to analyze the EIS spectra of the SS and DS. In this equivalent circuit model, R_s provides solution resistance, R_{ct} provides charge-transfer resistance, R_f provides resistance of the corrosion layer, Q_f and Q_{dl} represent the constant phase elements (*CPEs*) of the film capacitor and the electrostatic double layer capacitor, respectively [48]. The impedance of *CPE* can be calculated by the equation [59]:

$$Z_{CPE}=\frac{1}{Y_0(jw)^n} \quad (1)$$

Where Y_0 is the coefficient, j is the imaginary, w is the angular frequency, and n is the phase. Because of the non-ideal capacitance characteristics of the electrode surface, *CPE* is considered to be an alternative to capacitance.

In the low-frequency region of the Nyquist plot, the kinetics of electrochemical reactions are restrained by diffusion, resulting in a frequency-dependent response that is represented as a straight line with a constant slope, commonly known as the Warburg straight line [60]. Thus, a Warburg element (W) was appended to the circuit of the BS for analysis, as shown in Figure S4b.

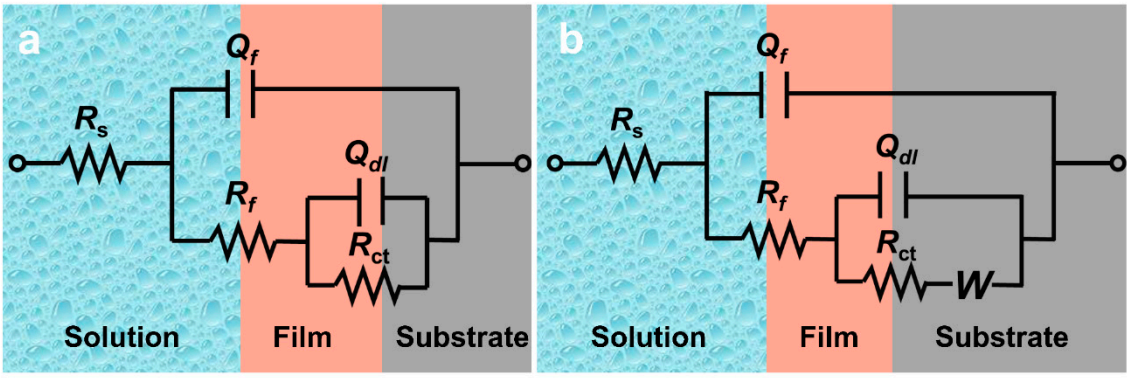

Figure S4. Equivalent circuits for the EIS results of the (**a**) SS and DS, (**b**) BS.

References

58. Wang P, Zhang D, Qiu R, Wu JJ. Super-hydrophobic metal-complex film fabricated electrochemically on copper as a barrier to corrosive medium. Corros Sci 2014;83:317-26.

48. Wang P, Chen XT, Li TP, Cai HY, Zhang D. Exceptional atmospheric corrosion inhibition performance of super-hydrophobic films based on the self-propelled jumping behavior of water droplets. Corros Commun 2021;1:40-6.
59. Wang P, Zhang D, Qiu R. Liquid/solid contact mode of super-hydrophobic film in aqueous solution and its effect on corrosion resistance. Corros Sci 2012;54:77-84.
60. Liu F, Shan DY, Song YW, Han EH, Ke W. Corrosion behavior of the composite ceramic coating containing zirconium oxides on AM30 magnesium alloy by plasma electrolytic oxidation. Corros Sci 2011;53:3845-52.